Journal of Structural Biology 191 (2015) 156–164

Contents lists available at ScienceDirect

Journal of Structural Biology

journal homepage: www.elsevier.com/locate/yjsbi

Dormant *Bacillus* spores protect their DNA in crystalline nucleoids against environmental stress

Christin Dittmann [a,1], Hong-Mei Han [b,1], Markus Grabenbauer [b,2], Michael Laue [a,*]

[a] Advanced Light and Electron Microscopy (ZBS 4), Robert Koch Institute, Nordufer 20, D-13353 Berlin, Germany
[b] Department of Systemic Cell Biology, Max-Planck-Institute of Molecular Physiology, Otto-Hahn-Strasse 11, D-44227 Dortmund, Germany

ARTICLE INFO

Article history:
Received 22 December 2014
Received in revised form 10 June 2015
Accepted 18 June 2015
Available online 19 June 2015

Keywords:
Spore
Nucleoid
DNA
CEMOVIS
Crystal
Resistance

ABSTRACT

Bacterial spores of the genera *Bacillus* and *Clostridium* are extremely resistant against desiccation, heat and radiation and involved in the spread and pathogenicity of health relevant species such as *Bacillus anthracis* (anthrax) or *Clostridium botulinum*. While the resistance of spores is very well documented, underlying mechanisms are not fully understood. In this study we show, by cryo-electron microscopy of vitreous sections and particular resin thin section electron microscopy, that dormant *Bacillus* spores possess highly ordered crystalline core structures, which contain the DNA, but only if small acid soluble proteins (SASPs) are present. We found those core structures in spores of all *Bacillus* species investigated, including spores of anthrax. Similar core structures were detected in *Geobacillus* and *Clostridium* species which suggest that highly ordered, at least partially crystalline core regions represent a general feature of bacterial endospores. The crystalline core structures disintegrate in a period during spore germination, when resistance against most stresses is lost. Our results suggest that the DNA is tightly packed into a crystalline nucleoid by binding SASPs, which stabilizes DNA fibrils and protects them against modification. Thus, the crystalline nucleoid seems to be the structural and functional correlate for the remarkable stability of the DNA in bacterial endospores.

1. Introduction

Bacilli and Clostridia can survive unfavourable conditions like starvation or aridity by intracellular production of survival stages called endospores (Dworkin and Shah, 2010). Such spores are extremely resistant against a wide range of harsh treatments, including high temperatures, desiccation and ultraviolet radiation, which ensures that the bacteria survive even extreme environmental conditions (reviewed by Setlow, 2007). Some species cause infectious diseases in humans that are mainly related with the transmission or survival of spores (Mallozzi et al., 2010). The most prominent is the infection by spores of *Bacillus anthracis* which can cause various forms of anthrax disease (Dixon et al., 1999). Moreover, environmental stability and ease of production were the main reasons why spores of *B. anthracis* have been used as bioweapons (Pohanka and Kuca, 2010) and still are considered as a relevant threat (Lane et al., 2001; Bossi et al., 2006).

The remarkable resistance of the bacterial spore is generated by a couple of features which are acquired during sporulation. The bacterial DNA is copied and the copy is enclosed into a membrane-bound core, which is only permeable for some small molecules and ions including water (Cortezzo and Setlow, 2005; Ghosal et al., 2010; Bassi et al., 2012). A complex coat structure surrounds the core which retains large molecules and provides mechanical stability (Driks, 2002; Henriques and Moran, 2007; McKenney et al., 2013). The core plasma is loaded with high concentration of dipicolinic acid (associated with calcium ions at equal molarity) and small acid soluble proteins (SASPs) while a considerable amount of the water (up to 75% wet weight) is removed (Setlow, 2007). Studies using mutants and anti-sense RNA demonstrated that the presence of high concentration of SASPs is the key factor for providing resistance against UV, wet heat and desiccation (for a review see Setlow, 2007). SASPs bind to DNA *in vitro* (Nicholson et al., 1990) and most likely also *in vivo* (Francesconi et al., 1988; Setlow et al., 1991; Ragkousi et al., 2000). Binding of SASPs to DNA introduces a change in conformation of the DNA *in vitro* (Mohr et al., 1991; Frenkiel-Krispin et al., 2004; Setlow, 2007; Lee et al., 2008), which could account for the differences observed in UV-photochemistry (Donnellan and Setlow, 1965;

* Corresponding author.
E-mail address: lauem@rki.de (M. Laue).
[1] These authors contributed equally.
[2] Present address: Institute for Anatomy and Cell Biology, University of Heidelberg, Im Neuenheimer Feld 307, D-69120 Heidelberg, Germany.

http://dx.doi.org/10.1016/j.jsb.2015.06.019
1047-8477/

Setlow, 1995) and causes bundling of DNA, both *in vitro* and *in vivo* (Francesconi et al., 1988; Setlow et al., 1991; Frenkiel-Krispin et al., 2004). Based on these data, models have been proposed to explain how the conformational changes and DNA bundling can promote a protection of the spores (Frenkiel-Krispin et al., 2004; Frenkiel-Krispin and Minsky, 2006; Lee et al., 2008). However, the situation in spores might be more complex, because other molecules than DNA and SASPs could be involved (Setlow, 2007).

We investigated the ultrastructure and topochemical composition of spores from various species. As our main model we employed spores of *B. subtilis* to find out about the relevance of their particular architecture for dormancy and resistance. By using advanced methods of ultrastructural research, such as cryo-electron microscopy of vitreous sections (CEMOVIS; Al-Amoudi et al., 2004), we were able to find structural features which have not been described before. In the present paper we describe that the DNA of dormant *Bacillus* spores is arranged in a crystalline nucleoid which is only formed in the presence of major SASPs and which is unpacked early in germination at a time where resistance of the spore is lost. Both results suggest that the crystalline arrangement of the DNA is responsible for the remarkable resistance of the spores. Investigation of spores from the genera *Geobacillus* and *Clostridium* indicate that the nucleoid structure is similar to that of *Bacillus* spores which let us hypothesize that a crystalline nucleoid might be a general feature of all dormant endospores.

2. Materials and methods

2.1. Bacterial strains and spore preparation

Bacillus subtilis ATCC 6633, *B. subtilis* 168, *B. subtilis* PS356 (*sspA*$^{-}$*sspB*$^{-}$; Mason and Setlow, 1986), *B. subtilis* PS482 (*sspA*$^{-}$*sspB*$^{-}$*sspE*$^{-}$ Cm; Hackett and Setlow, 1988) and *Bacillus thuringiensis* DSM 350 were grown over night on tryptic soy agar (TSA) or Luria–Bertani (LB) agar at 37 °C.

For spore preparation, the cells of vegetative bacteria were cultivated in 100 ml LB or tryptic soy broth (TSB) liquid medium over night at 37 °C using a shaker at 200 rpm. Sporulation was induced by adding 50 ml of the cell suspension to 500 ml sporulation medium. The medium was prepared as described (Sterlini and Mandelstam, 1969) with slight modification: 0.0722 g $FeCl_2 * 4H_2O$, 9.829 g $MgSO_4 * 7H_2O$, 0.0126 g $MnCl_2$, 0.535 g NH_4Cl, 0.106 g Na_2SO_4, 0.068 g KH_2PO_4, 0.0965 g NH_4NO_3, 0.29 g $CaCl_2 * 2H_2O$, 0.2 g L-glutamic acid and 0.02 g L-tryptophan in a final volume of 1000 ml prepared with distilled water. The pH was adjusted to 7.1.

Cells were sporulated for 11–13 days at 37 °C. Controls of the sporulation process were conducted using a phase contrast microscope (Axiophot; Carl Zeiss Microscopy GmbH). Spores appear as bright ovoid spheres in contrast to the dark, rod-shaped vegetative cells or debris. Separating of spores from vegetative bacteria and debris was done by centrifugation at 4 °C and washing in 0.05 M Hepes buffer (pH 7.2). The suspension was centrifuged for 10 min at 2000*g*. Supernatant was discarded and the pellets were washed three times by resuspension in 0.05 M Hepes and centrifugation for 20 min at 2000*g* and 4 °C. Spores were stored at 4 °C in 0.05 M Hepes.

Geobacillus stearothermophilus (NCIB 8923 = ATCC 12980) was grown on solid nutrient agar for 3 days at 56 °C and then moved to room temperature for sporulation. Formation of spores was monitored by phase contrast light microscopy and took several days. Spores were harvested using a Drigalski spatula, filtered through glass wool and washed three times with distilled water. Finally, spores were stored in 70% ethanol at 4 °C until use.

Spores of *B. anthracis* Sterne strain 34F2 and *Clostridium difficile* NCTC 13366 were produced according to a European standard procedure (prEN 14347:2001 [D]) and stored at 4 °C in double distilled water or in 70% ethanol until use.

Finally, all spore preparations were examined by phase-contrast microscopy to check the purity and physiological status of the spore population (fraction of phase-bright and phase-dark spores) to correlate possible variations in ultrastructure with the physiological status of the spores.

2.2. CEMOVIS

Spores of *B. subtilis* (ATCC 6633) in PBS, including 30% dextran (approx. 40 kDa, Sigma–Aldrich, Germany), were taken up into copper tubes (Goodfellow GmbH, Germany) and frozen by self-pressurized rapid freezing as described previously (Han et al., 2012). For cryo-sectioning, the tube was mounted at a pre-cooled (−150 °C) EM FC6 cryo-ultramicrotome (Leica Microsystems, Germany) and trimmed to a rectangular shaped block (70–100 μm base and approx. 100 μm height) using a 20° Cryotrim diamond knife (CT1303; Diatome, Switzerland). Ribbons of cryo-sections were produced with a cryo-immuno diamond knife (25°; Diatome) as described (Han et al., 2008) and attached to pre-cooled 600 mesh EM grids with an eyelash using electrostatic charging (EM CRION, Leica Microsystems).

Grids were loaded in a pre-cooled cryo-specimen holder (Gatan 626-DH; Gatan, USA) and transferred into a cryo-electron microscope (JEOL JEM-1400; JEOL Germany, Germany). Microscopy was performed at −178 °C using an acceleration voltage of 120 kV and micrographs were recorded with a 4 K × 4 K CMOS camera (F-416; TVIPS, Germany). Vitrification of frozen sections was confirmed by electron diffraction. The electron dose on the specimen was kept between 700 and 1500 e^-/nm^2. Some images were taken with a JEOL JEM 3200FSC electron microscope equipped with a field-emission gun at an operation voltage of 200 kV. An in-column omega energy filter was used with a slit width of 25 eV. Micrographs were recorded with a K2 Direct Detection Camera (Gatan, Inc., Pleasanton, CA) under minimal dose conditions. Fast Fourier transforms (FFTs) were calculated using DigitalMicrograph (Gatan, Inc., Pleasanton, CA) and periodicity of striations in crystalline core regions was established by measuring the distance between spots in the power spectrum of the FFT.

2.3. Chemical fixation and resin embedding for thin section transmission electron microscopy

Spore suspensions were fixed in 10% formaldehyde (produced from paraformaldehyde by heating to 70 °C for 30 min) and 0.05% (v/v) glutaraldehyde in 0.05 M Hepes buffer (pH 7.2) for 5 min at room temperature in a 2 ml reaction tube. Subsequently, the tube was transferred to a particular microwave oven (Rapid Electron Microscopy Tissue Processing System; Milestone, Italy) using the Histomodule F/H that was filled with distilled water to complete fixation. Within the oven, suspensions were heated for 2 min from room temperature to 37 °C, followed by 2 min from 37 °C to 50 °C and finally for 1 min at 50 °C using a setting of 15% of the microwave power (120 W) and a stirrer to move the water which surrounded the sample vials.

To facilitate embedding, spores were centrifuged for 10 min at 2000 g and the pellet was resuspended in the same volume of 3% low-melting point agarose (Sigma–Aldrich, Germany). In order to produce thin gels the mixture was filled between two microscopic slides that were separated with 0.3 mm spacers and placed one ice. Small agarose slices (1 × 2 mm) were isolated and transferred into 0.05 M Hepes for 10 min at RT. Dehydration and embedding in LR White (The London Resin Corp., United Kingdom) were conducted

as described (Laue et al., 2007) but with slight modifications. Samples were dehydrated in an ethanol series (70% for 10 min and 100%, two times for 5 min) and infiltrated by an 1:1 mixture of LR White/absolute ethanol for 5 min followed by pure LR White, twice for 5 min and 10 min. Samples were transferred to an airfuge (Beckman, USA) tube (240 µl), mixed with pure LR White including accelerator (5 µl per ml monomer), covered with the top of a gelatine capsule and polymerized for one hour on ice. Finally, samples were stored at 60 °C over night which removed unpolymerized resin.

For immunolabeling experiments, spores were fixed and transferred into low-melting point agarose as described above but embedded in Lowicryl K4M (Polysciences, USA) at low temperature (−35 °C) (Fuchs et al., 2003). Briefly, samples were dehydrated in a series of ethanol while lowering the temperature stepwise to −35 °C (progressive lowering of temperature, PLT method). Infiltration with Lowicryl resin was done by using mixtures of ethanol and resin and finally with pure resin. Polymerization of Lowicryl-embedded samples was conducted by ultraviolet light at −35 °C (1 day) and 0 °C (1 day). The whole preparation was carried out in an automatic freeze-substitution device (AFS 2, Leica Microsystems, Germany).

Embedded samples were trimmed with a milling machine (Leica EM RAPID; Leica Microsystems) and ultrathin sections (70–80 nm) were cut using an ultramicrotome (Leica EM UC7; Leica Microsystems). Ultrathin sections were placed on a slot grid that was covered with a polymer film (pioloform F). Sections were stained with a solution of 1.8% uranyl acetate and 0.1% methyl cellulose (w/v; Sigma–Aldrich) for 10–20 min (Roth et al., 1990). Ultrathin sections were examined using a transmission electron microscope (Tecnai 12 Spirit; FEI, The Netherlands) at 120 kV and images were recorded with a CCD camera, either at a resolution of 1376 × 1024 pixels (Megaview III; Olympus SIS, Germany) or 4096 × 4096 pixels (Eagle; FEI Corp., The Netherlands). FFTs were calculated using the iTEM software (Olympus SIS, Germany) and periodicity of striations in crystalline core regions was established by measuring the distance between spots in the power spectrum of the FFT.

2.4. Immunolabeling

Ultrathin sections of the Lowicryl K4M samples were incubated on 30 µl droplets (section facing down) at room temperature using the following protocol: 2.5% glutaraldehyde in phosphate-buffered saline (PBS) for 2 min (the fixation of the section improves the stability of the spore core within the section); four times washing with PBS; two times glycine (50 mM) in PBS for 5 min; blocking solution (contains 0.5% fish gelatin, 0.5% bovine serum albumin [protease free; T844.1; Carl Roth GmbH, Germany], and 0.01% Tween 20 [Fisher Scientific] in PBS) for 1 min; blocking solution for 30 min; primary antibody diluted in blocking solution for 60 min; six times blocking solution for 5 min each; secondary antibody in blocking solution for 60 min; two times blocking solution for 5 min each; glycine (50 mM) in PBS for 5 min; two times PBS for 5 min each; six times distilled water. As primary antibodies we used two different monoclonal mouse antibodies against double stranded DNA (HYB331-01; abcam, United Kingdom; MAB030; Millipore, Germany) and as a control a monoclonal mouse antibody against green fluorescent protein. The secondary antibody was a goat anti-mouse IgG (H&L) that was coupled to 5 nm gold (British Biocell International, United Kingdom).

2.5. Germination of spores

To analyze germinating spores, several batches of *B. subtilis* ATCC 6633 ($1 * 10^8$ spores per batch in water) were dried for 4 h at 37 °C and activated by adding 1 ml TSB to each of the batches at 37 °C in a thermo-mixer (700 rpm). At constant time intervals of 5 min batches were fixed chemically as described above (one batch of activated spores per time point). The time course of activation was assessed over time by phase-contrast light microscopy as a change of the spore's refraction: dormant spores are phase-bright and activated spores are phase-dark particles. For microscopy, 5 µl of the fixed suspension were transferred on a microscope slide, dried for one hour and covered with 10% polyvinyl pyrrolidone K 90 and a cover slip. Samples were viewed by phase-contrast light microscopy (Axiophot; Carl Zeiss Microscopy GmbH) and the fraction of dark, i.e. activated spores, was determined and plotted over time.

3. Results

In vitreous cryo-sections through the core region of dormant *B. subtilis* spores we found locally confined striation patterns, which resembled crystal lattices (Fig. 1A–C). The spacing of the striations was 4.1 nm (SD = 0.31 nm, $n = 14$ spore cross sections) as determined by calculation of FFTs. To facilitate a further analysis, including immunogold labeling and investigation of risk group level 2 organisms, such as *B. anthracis* Sterne, we tried to find the crystalline structures also in samples which were processed at ambient temperature. This became possible by using a microwave-assisted chemical fixation in combination with a rapid embedding in an acrylate resin (LR White) and finally a contrasting of sections through a sort of negative staining (Laue et al., 2007). Inspection of such sections at higher resolution revealed parallel striation pattern, like those found by CEMOVIS, and sometimes regularly spaced dots in confined regions of the core (Fig. 2A, B) which suggest that the structural features could represent crystalline objects that were either sectioned longitudinally or in cross-section. The spacing of the parallel striation pattern in plastic sections was about 3.5 nm (SD = 0.09 nm, $n = 10$ cross-sections of spores) which is smaller than the spacing established for the corresponding pattern visualized by CEMOVIS, but to be expected because of the shrinkage of structures in plastic-embedded biological material (Luft, 1973; Eisenberg and Mobley, 1975). In longitudinal sections through the spore core the regular striation pattern regularly was found in an electron dense band which usually followed the core membrane (Fig. 2C, D) and resembled the ring-like nucleoid structures found by fluorescence microscopy (Ragkousi et al., 2000; Frenkiel-Krispin and Minsky, 2006).

To explore if the striation pattern is associated with the presence of DNA as the major constituent of the nucleoid, we performed immunolabeling studies using anti-DNA antibodies. Our results clearly show that anti-DNA labeling is predominantly associated with the striation pattern within the core rather than with other regions of the core plasma (Fig. 3A, Supplementary Fig. 1A). Specific labelling could be demonstrated with two independent antibodies against DNA while controls with nonsense antibodies never showed the same labeling pattern (Supplementary Fig. 1), indicating presence of DNA in the striated core regions. In the next experiment we tried to illuminate the fate of the DNA-containing core regions during spore germination. For time course, spores were activated by mixing with a nutrient-rich culture medium (tryptic soy broth) at 37 °C and every 5 min a sample was chemically fixed. The activation of germination was assessed by phase-contrast light microscopy as a change from phase-bright to phase-dark appearance which indicates uptake of water into the core (Kong et al., 2011). In our germination assay, the appearance of most spores changed between 5 and 15 min after mixing with the medium (Supplementary Fig. 2). During this period the distinct striation pattern within the core started to lose its highly ordered

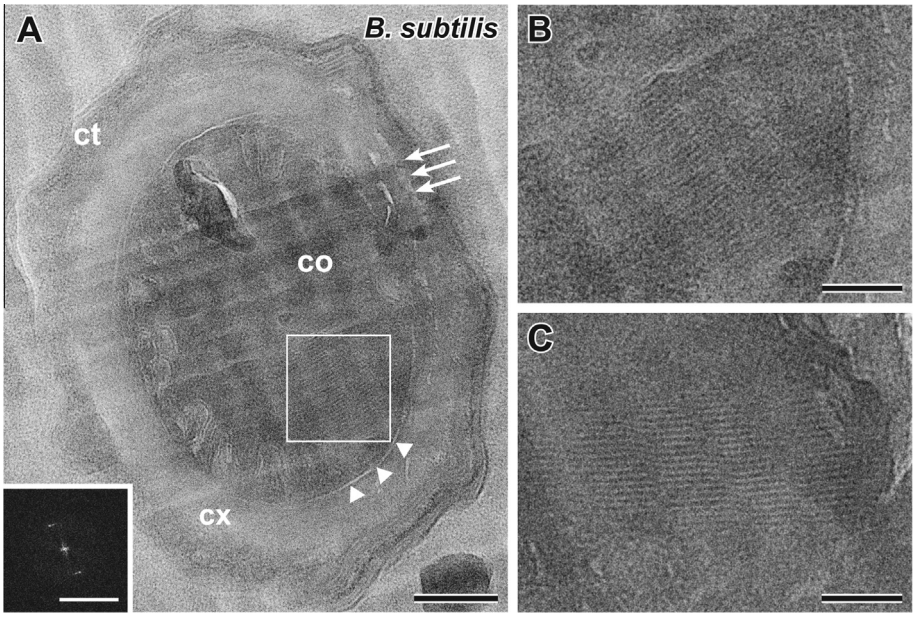

Fig. 1. Crystalline core regions in thin sections through dormant spores of *Bacillus subtilis* visualized by cryo-electron microscopy of vitreous sections (CEMOVIS). The spore core (*co*) reveals highly ordered structural arrangements, in form of parallel striations, which appear crystalline. (A) Cross-section through a dormant spore. The white box indicates a region of the core which shows characteristical striations (a higher magnification of this region is shown in B). The power spectrum of the FFT calculated for this core region (inset) shows distinct peaks. Arrows indicate the direction of sectioning. (B, C) Higher magnification of striated core regions in two different spores. *ct* = coat, *cx* = cortex, *arrowheads* = core membrane; Bar in A = 100 nm, in B, C = 50 nm, inset = 0.5 1/nm.

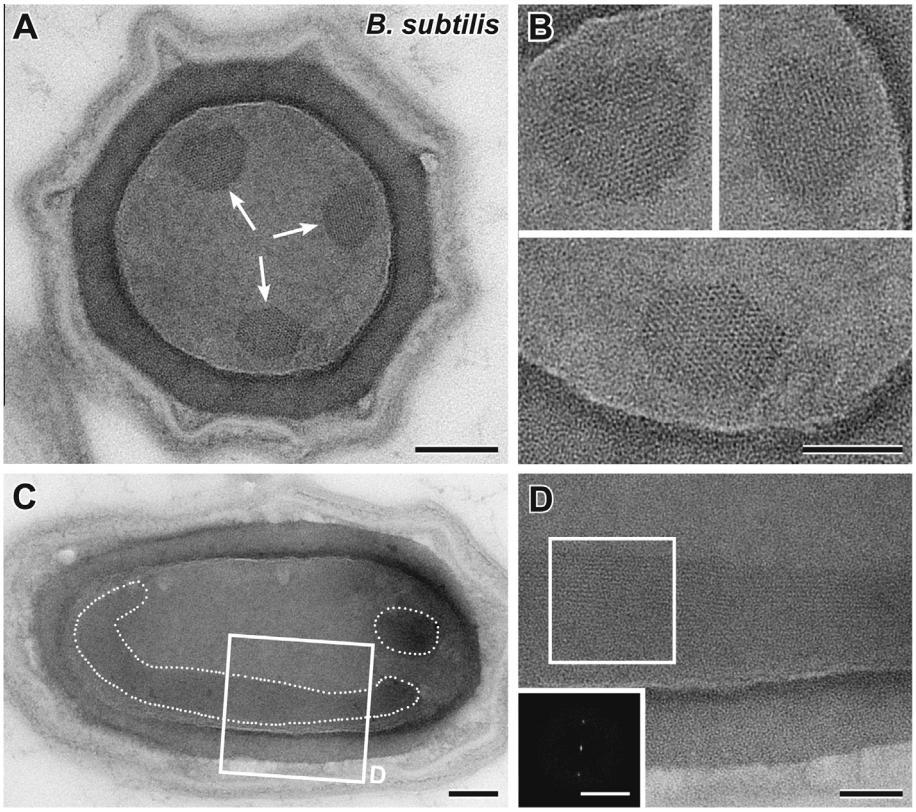

Fig. 2. Crystalline core regions in thin sections through dormant spores of *Bacillus subtilis* visualized by conventional transmission electron microscopy after chemical fixation and resin embedding. (A, B) Cross-section through a spore with three crystalline regions (*arrows*) which show parallel striations, spaced dots or a mixture of both structural elements (B shows the three core regions at higher magnification) representing different orientations of the highly ordered structures relative to the section plane. (C, D) Longitudinal section through a dormant spore. The striated regions of the core (labeled with a dotted line in C and depicted at higher magnification in D) are continuous and extend as ribbons throughout the spore core resembling the nucleoid. The inset in D shows the power spectrum of the FFT calculated for the region marked with a box. Bar in A, C = 100 nm, in B, D = 50 nm, inset = 0.5 1/nm.

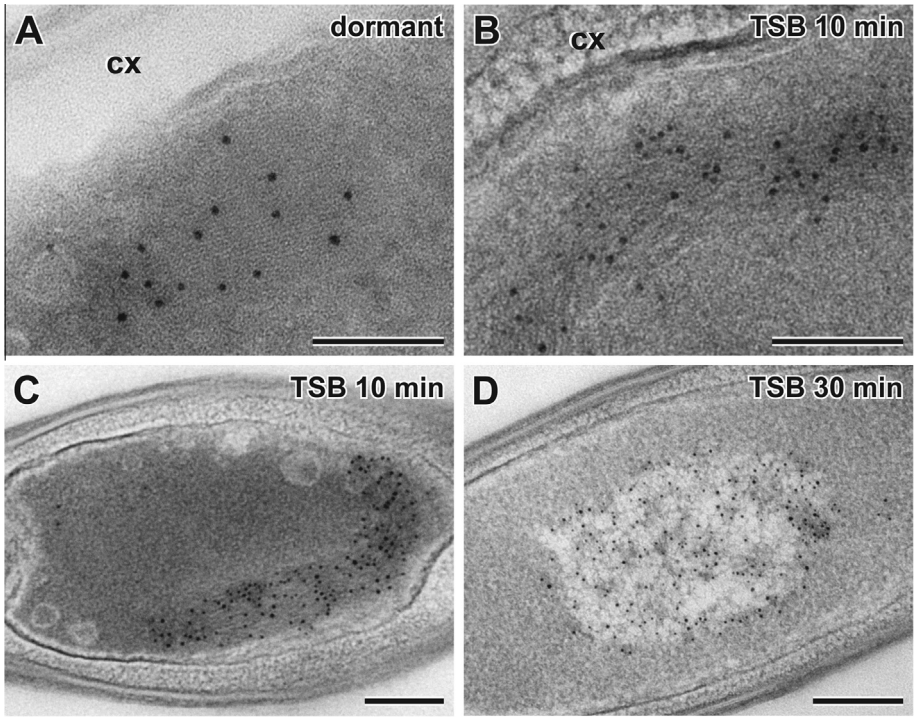

Fig. 3. Immunogold labeling of sections through spores of *Bacillus subtilis* with antibodies against DNA (*anti-DNA*). (A) Gold labeling is associated with a striated core region in a dormant spore. (B) In a germinating spore (10 min after addition of tryptic soy broth, *TSB 10 min*), labeling for DNA is associated with bundles of more or less parallel arranged fibers which however lack a distinct spacing. Note that the cortex (*cx*) of the spore has already changed its structural appearance from homogenous (A) to granular (B), which represents lysis of the cortex and is an indication for early germination (Santo and Doi, 1974). (C, D) Longitudinal sections through spores that were fixed either 10 min (*TSB 10 min*) or 30 min (*TSB 30 min*) after addition of TSB. (C) After 10 min, the gold-labeled fibers cover a similar domain within the core than the striated core regions of dormant spores (compare Fig. 2C, D). (D) After 30 min, gold labeling is confined to the centre of the core decorating aggregates of short fibers within a loosened cytoplasm. Bars = 100 nm.

organization (i.e. the distinct spacing), which is indicated by the presence of spores showing bundled fibers instead of the striation pattern in comparable core regions. Moreover, the fiber bundles were densely labeled by anti-DNA antibodies (Fig. 3B, C), suggesting that these structures correspond to the formerly highly ordered striated regions of the core in dormant spores. At later time points ($\geqslant$20 min) the anti-DNA positive fibers were more and more separating. Finally the fibers cover a more or less central part of the core plasma which was devoid of ribosomes (Fig. 3D) and which represents the typical structure of the nucleoid in chemically fixed bacteria (Eltsov and Zuber, 2006). Note that studies using high pressure freezing and freeze-substitution were not successful with dormant spores in many attempts, most probably because fixatives and resin could not enter the spore core during freeze-substitution and resin infiltration which is in line with the observation that an intact core membrane seems to be the relevant molecular barrier if it remains undisturbed (Cowan et al., 2004; Cortezzo et al., 2004). However, high-pressure freezing and freeze-substitution of activated spores at early points of germination (from about 5 min on after adding of TSB) proved to be successful and showed a similar bundling of fibers at early stages of germination as did spores prepared by chemical fixation (Supplementary Fig. 3) which indicates that bundled fibers are not an artifact of the chemical processing of the samples.

Our data suggest, that in dormant spores, DNA is organized in a highly ordered, crystalline fashion which is lost during germination at a time, where the core is rehydrating by water uptake. This dramatic change is associated with a loss of resistance of the spore against a couple of treatments (e.g. heating, UV radiation) (Setlow, 2007). The resistance providing key factor, is the presence of small acid soluble proteins (SASPs), because differences in the spore's water or dipicolinic acid content did not fully account for the observed resistance (Setlow et al., 2006; Setlow, 2007). Spores of mutants, in which most of the SASPs have been knocked out, are much more susceptible to environmental stress than spores of the corresponding wild-type (Setlow, 2007). Several studies demonstrated that SASPs are binding to DNA of spores (Francesconi et al., 1988; Nicholson et al., 1990; Frenkiel-Krispin et al., 2004; Lee et al. 2008) which suggests that this binding may protect the DNA somehow. To verify whether the presence of SASPs is necessary to generate the crystalline arrangement of DNA-containing core regions, we analyzed SASP-minus mutants of *B. subtilis* and their corresponding wild-type. While the wild-type showed the typical striation patterns in their cores, SASPs-minus mutants were, without exception, devoid of a comparable striation pattern (Fig. 4). This result indicates that SASPs are necessary to form highly ordered, crystalline core regions which contain DNA.

In the next step we wanted to explore whether the presence of crystalline core regions is a general feature of the spores from endospore-forming bacteria. Firstly, we investigated dormant spores of other *Bacillus* species, such as *B. anthracis* and *B. thuringiensis*. The characteristic striation pattern was regularly found in their core (Fig. 5; Supplementary Fig. 5). While the striation pattern was most prominent in spores of *B. subtilis*, nucleoids of other *Bacillus* species showed this regular pattern less clearly as revealed by the FFTs (i.e. distinct spots in the power spectra were faint) but with the same characteristics, like a lattice space of 3.3 nm (*B. anthracis* and *B. thuringiensis*; $n = 10$ spore sections per species) which is close to the value measured for *B. subtilis* (3.5 nm). Preliminary investigations of spores from the genetically more distant *G. stearothermophilus* and *C. difficile* also

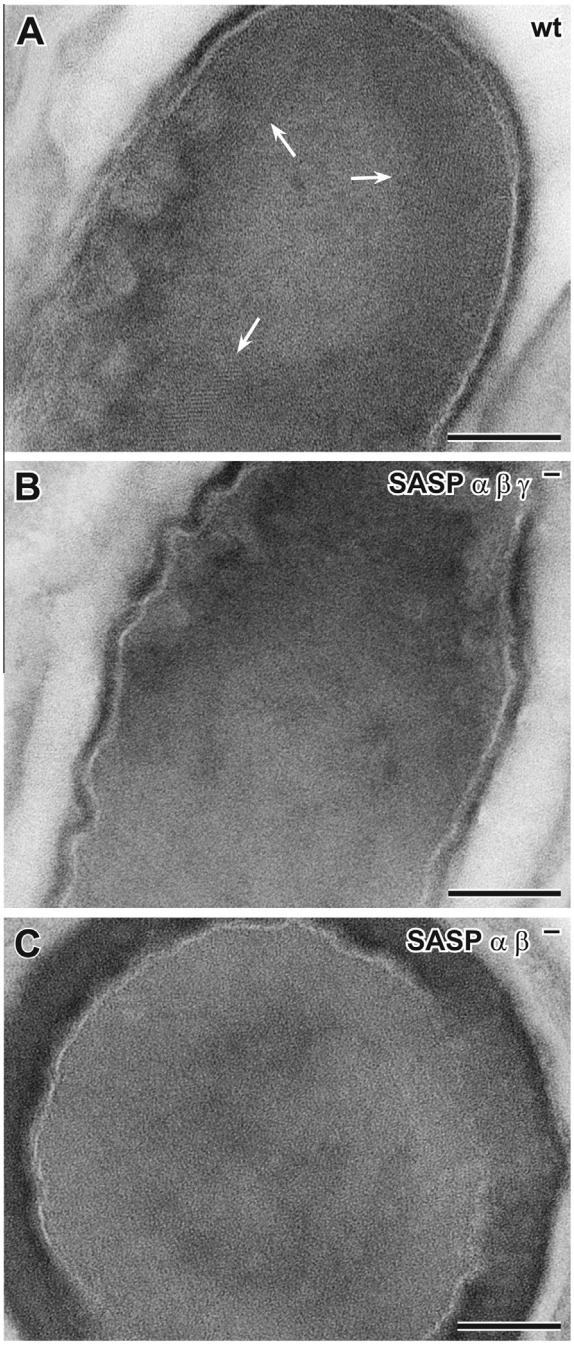

Fig. 4. Comparison between dormant spores of wild-type (wt) *B. subtilis* 168 (A) and spores of mutants of this strain lacking α/β-type SASP and SASP-γ (*SASP* $\alpha\beta\gamma^-$) (B) or α/β-type SASP (*SASP* $\alpha\beta^-$) (C). While the core of the wild type spore reveal striated nucleoid structures (*arrows*) the spores of mutants are devoid of comparable ordered structures. Bars = 100 nm.

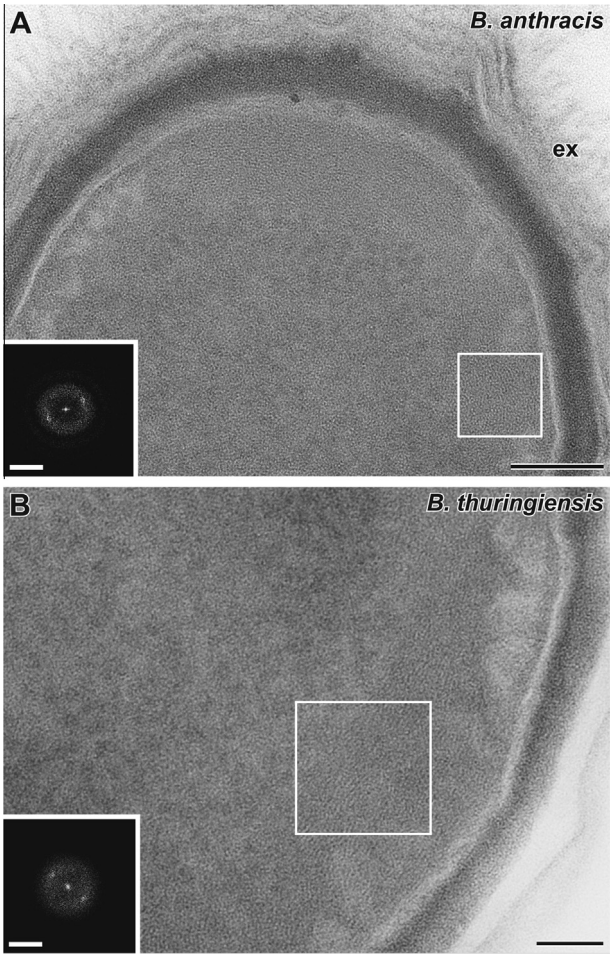

Fig. 5. Crystalline core structures are detectable in spores of *Bacillus anthracis* (A) and *Bacillus thuringiensis* (B). Insets are showing the power spectrum of the FFT calculated for the respective core region marked with a box. The entire core of the *B. thuringiensis* spore is shown in Supplementary Fig. 5. *ex* = exosporium. Bar in A = 100 nm, in B = 50 nm and in the insets = 0.5 1/nm.

demonstrated regularly the presence of a faint striation pattern in the nucleoid region of the spore core which appeared qualitatively similar to the pattern observed in *Bacillus* spores (Supplementary Fig. 4).

4. Discussion

Our data strongly suggest that the DNA in *Bacillus* spores is packed into a crystalline nucleoid, which is depending on the presence of SASPs. Mutants, which do not express all relevant SASPs, as well as late stages of germination, in which SASPs are soluble and degrading (Setlow, 2007), lack the highly ordered core structures. Published data support this notion. SASPs are localized in ring-like nucleoid structures (Francesconi et al., 1988; Ragkousi et al., 2000) that resemble the elongated core structures showing a crystalline striation pattern in longitudinal sections through spores. The addition of SASPs to DNA *in vitro* (Frenkiel-Krispin et al., 2004) or the heterologous expression of SASPs in *E. coli* (Setlow et al., 1991) induced the bundling of DNA, which is a necessary pre-requisite to generate crystalline packing of molecules. Periodicity of the striation pattern visualized by CEMOVIS is larger (4.1 nm) than the periodicity of the lattice pattern found for packed double-stranded DNA in bacteriophages and viruses (2.5 nm, Lepault et al., 1987; 2.6 nm, Booy et al., 1991), supporting the idea of a tight packing of DNA mediated by SASPs *in vivo*.

While the molecular arrangement of the DNA/SASP interaction has been analyzed *in vitro* by CEMOVIS (Frenkiel-Krispin et al., 2004) and by revealing the crystal structure (Lee et al. 2008), the situation *in vivo* was unclear. Binding of SASPs to DNA introduce conformational changes *in vitro* (Mohr et al., 1991; Frenkiel-Krispin et al., 2004; Lee et al., 2008) that could allow efficient packaging of DNA/SASP filaments *in vivo* (Frenkiel-Krispin et al., 2004). To explain the observed periodical striation pattern in this study we propose a simple model which is based on the packaging analysis provided by Frenkiel-Krispin et al. (2004). DNA/SASP filaments are tightly packed by parallel and

anti-parallel filament orientation as well as by rotation in length axis to provide maximal interdigitation between the SASPs of neighboring filaments. If such filament bundles are viewed in cross-section, they show characteristical periodical arrangements (one filament is surrounded by six other filaments) of filament columns (Fig. 6). The width of a filament is between 5.1 nm (crystal structure; Lee et al., 2008) and 5.5 nm (CEMOVIS; Frenkiel-Krispin et al., 2004). If we assume a difference in electron density between the core of the filament, where the DNA is situated, and periphery, which is covered by the SASP shell, electron beam illumination perpendicular to the filament axis would generate a periodical striation pattern which has a smaller period than the filament size and which is in the range of the periodicity observed in our study by using CEMOVIS (Fig. 6). Our assumption of a difference in electron density between core and shell regions is likely because the protein masses are dense, especially if they are interdigitating between neighboring filaments, like the packaging analysis of Frenkiel-Krispin et al. (2004) suggests. However, even if the density would be inverted (i.e. core denser than periphery), the model can explain the observed striation pattern, because it would only switch gray and white stripes but not the periodicity of the pattern. Thus, our findings are in line with the data obtained *in vitro* and imply that DNA/SASP filaments are tightly packed in a crystalline arrangement *in vivo*.

The differences of the lattice periodicity between ice embedded (CEMOVIS) and plastic (LR White) embedded samples is most likely due to the expected shrinkage of samples during plastic embedding (Luft, 1973; Eisenberg and Mobley, 1975). However, the contrast in sections of plastic-embedded samples is generated by the heavy metal ions bound to material in the section and is different from the contrast in samples visualized by CEMOVIS (Dubochet et al., 2007), which might have an additional influence on the measurements. As pointed out in the result section, visualization of the striation pattern in plastic section was only possible by using hydrophilic acrylate resin in conjunction with the particular on-section staining (uranyl acetate/methyl cellulose) suggested by Roth et al. (1990). This staining seems to work as a mixture between negative and positive staining, which is documented by the bright appearance of the core biomembrane and high density of the cortex. However, it is unclear how exactly this staining has generated the contrast that was observed. In cross-section of nucleoids a pattern of black dots (surrounded by less dense material) is visible that shows a similar arrangement as the filaments in our model (compare Fig. 2B with Fig. 6) which could be due to staining of the DNA filaments.

Chemical fixation and plastic embedding was used to allow immunolabeling studies and to analyze spores of species which belong to biosafety risk group level 2. It is well known that such preparation methods introduce changes to the samples which are difficult to detect without proper controls and which depend on the preparation conditions and the object. For *B. subtilis* spores, we show that the chemically fixed plastic embedded samples reveal similar structures as the corresponding spores visualized by CEMOVIS, which suggests that the chemical preparation methods preserve structures of interest at a reasonable quality. However, this must not necessarily be the case for the other species studied. The visibility of the core striations is less clear in other species than in *B. subtilis* which might be due to less efficient stabilization of the regular arrangement of DNA/SASP filaments by chemical fixation. However, although core striations appear

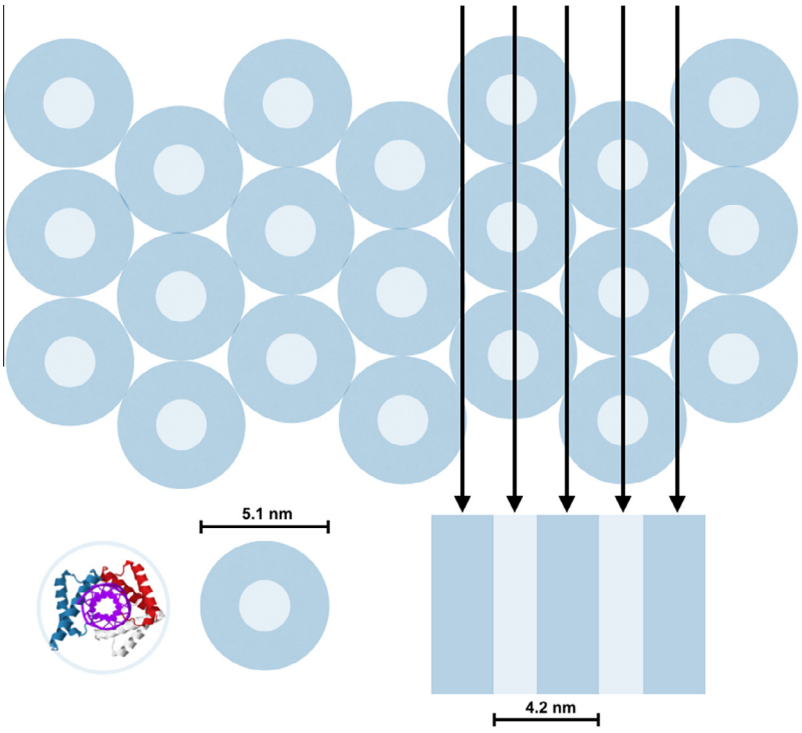

Fig. 6. A simple model of DNA/SASP-filament packing which explains the observed striation pattern of crystalline core regions in dormant spores. Each filament is represented as a circular envelope of the projection of the molecular model from the crystal structure (Lee et al., 2008; PDB structure ID: 2Z3X) viewed in length axis (i.e. axis of the DNA helix). The corresponding molecular visualization of the crystal structure is shown at the lower left (DNA helix in pink). Filaments are packed at maximal density as suggested by in silico packing analysis of Frenkiel-Krispin et al. (2004, Fig. 3). In this model one filament is surrounded by six filaments achieving maximum interdigitation between neighboring filaments if three of six filaments in average were oriented in antiparallel configuration and if filaments are axially rotated to give the best fit. In such a configuration the DNA is localized in the centre of each filament, rotated at various angles and protein masses are surrounding it. The diameter of each filament, according to the crystal structure, is about 5.1 nm. To explain the observed striation pattern generated by electron beam illumination (arrows) in such a model, only a difference in electron density between filament core (DNA) and periphery (protein) has to be assumed, regardless of their actual distribution (centre denser than periphery or vice versa). The resulting periodicity of the striation pattern in the model is smaller than the diameter of the filament (4.2 versus 5.1 nm) which corresponds to the observed periodicity (4.1 nm). See text for further discussion.

noisier, they could be found in three *Bacillus* species, including anthrax, and in the more distantly related *G. stearothermophilus* and *C. difficile*. Based on these observations we hypothesize that the crystalline nucleoid in dormant spores is a general feature of the endospore-forming bacteria.

Further studies should employ CEMOVIS to analyze the crystalline core regions in other species than *B. subtilis* and compare their structure more accurately. Unfortunately, high-pressure freezing followed by freeze-substitution and resin embedding, which would be an appropriate method to facilitate the screening of various species, does not preserve the cores of dormant spores properly (cores appear not well infiltrated, are condensed and break during sectioning). The main reason for this fact is, that the core membrane of dormant spores is impermeable for most molecules (Cortezzo and Setlow, 2005; Ghosal et al., 2010; Bassi et al., 2012) and therefore considered as the main molecular barrier in spores (Cowan et al., 2004; Cortezzo et al., 2004). Resin monomers are most likely too big to cross this barrier and therefore are not infiltrating the core. A small fraction (below 5%) of each spore population can be sufficiently preserved by high-pressure freezing followed freeze-substitution and resin embedding. This fraction usually corresponds in number to the fraction of spores which appear phase-dark in phase-contrast light microscopy indicating that the spores are already germinating or are somehow impaired but not dormant. As a consequence, correlation between physiological status and structure is important and a direct correlation by correlative light and electron microscopy would be desirable.

The major function of the association of SASPs and DNA in dormant spores is to provide resistance against a couple of environmental factors (Setlow, 2007). Formation of highly ordered and tightly packed DNA is the structural and mechanistic correlate of this important fact. The presence of such an arrangement *in vivo* has been anticipated or deduced already by the studies on the interaction of DNA and SASPs *in vitro* (Frenkiel-Krispin et al., 2004; Lee et al. 2008). Bio-crystallization seems to be a strategy, at least in microorganisms, to survive hostile environmental conditions (Wolf et al., 1999; Minsky et al., 2002; Frenkiel-Krispin and Minsky, 2006). Besides energetic considerations (i.e. crystals are steady-state structures which need no energy after formation; Minsky et al., 2002), a crystalline structure provides superior stability against heat and non-ionizing radiation, since molecular movements (i.e. rotational, vibrational and intermolecular) are restricted. The analysis of the crystal structure of individual DNA/SASP filaments supports this notion because binding of SASPs to DNA enhances rigidity of the DNA (Lee et al., 2008).

Crystalline regions containing DNA may provide a structural hallmark for inactive DNA present under particular conditions, like starvation or hibernation (Minsky et al., 2002). Apart from those extreme situations, protection of "unused" DNA in highly specialized and differentiated cells seems to be plausible as well. Tight packing of DNA by protein/DNA-interaction may be one strategy to solve this issue, not only because of the rigidity provided, but also because a highly organized packing of DNA should facilitate DNA repair (Frenkiel-Krispin et al., 2004). Careful inspection of higher cells, especially in differentiated tissue or in dormant stages (e.g. hibernation) could help to clarify the question whether DNA bio-crystallization is a more widespread mechanism in biology to protect the genetic information from unwanted environmental interference.

Conflict of interest

The authors declare that there are no conflict of interests.

Transparency Document

The Transparency document associated with this article can be found in the online version.

Acknowledgements

We would like to thank Roland Grunow and Marc Thanheiser for providing spore suspensions and Christoph Schaudinn for critical reading of the manuscript. We declare no conflict of interests.

The study was funded by the German Ministry of Health and Max-Planck-Society.

Appendix A. Supplementary data

Supplementary data associated with this article can be found, in the online version, at http://dx.doi.org/10.1016/j.jsb.2015.06.019.

References

Al-Amoudi, A., Chang, J.J., Leforestier, A., McDowall, A., Salamin, L.M., Norleén, L.P., Richter, K., Blanc, N.S., Studer, D., Dubochet, J., 2004. Cryo-electron microscopy of vitreous sections. EMBO J. 23, 3583–3588. http://dx.doi.org/10.1038/sj.emboj.7600366.

Bassi, D., Cappa, F., Cocconcelli, P.S., 2012. Water and cations flux during sporulation and germination. In: Abel-Santos, E. (Ed.), Bacterial Spores. Claister Academic Press, Norfolk, pp. 143–167.

Booy, F.P., Newcomb, W.W., Trus, B.L., Brown, J.C., Baker, T.S., Steven, A.C., 1991. Liquid-crystalline, phage-like packing of encapsidated DNA in Herpes Simplex Virus. Cell 64, 1007–1015. http://dx.doi.org/10.1016/0092-8674(91)90324-R.

Bossi, P., Garin, D., Guihot, A., Gay, F., Crance, J.M., Debord, T., Autran, B., Bricaire, F., 2006. Bioterrorism: management of major biological threats. Cell. Mol. Life Sci. 63, 2196–2212. http://dx.doi.org/10.1007/s00018-006-6308-z.

Cortezzo, D.E., Koziol-Dube, K., Setlow, B., Setlow, P., 2004. Treatment with oxidizing agents damages the inner membrane of spores of *Bacillus subtilis* and sensitizes the spores to subsequent stress. J. Appl. Microbiol. 97, 838–852. http://dx.doi.org/10.1111/j.1365-2672.2004.02370.x.

Cortezzo, D.E., Setlow, P., 2005. Analysis of factors that influence the sensitivity of spores of *Bacillus subtilis* to DNA damaging chemicals. J. Appl. Microbiol. 98, 606–617. http://dx.doi.org/10.1111/j.1365-2672.2004.02495.x.

Cowan, A.E., Olivastro, E.M., Koppel, D.E., Loshon, C.A., Setlow, B., Setlow, P., 2004. Lipids in the inner membrane of dormant spores of *Bacillus* species are largely immobile. PNAS 101, 7733–7738. http://dx.doi.org/10.1073/pnas.0306859101.

Dixon, T.C., Meselson, M., Guillemin, J., Hanna, P.C., 1999. Anthrax. N. Engl. J. Med. 341, 815–826. http://dx.doi.org/10.1056/NEJM199909093411107.

Donnellan, J.E., Setlow, R.B., 1965. Thymine photoproducts but not thymine dimers found in ultraviolet-irritated bacterial spores. Science 149, 308–310. http://dx.doi.org/10.1126/science.149.3681.308.

Driks, A., 2002. Maximum shields: the assembly of the bacterial spore coat. Trends Microbiol. 10, 251–254. http://dx.doi.org/10.1016/S0966-842X(02)02373-9.

Dubochet, J., Zuber, B., Eltsov, M., Bouchet-Marquis, C., Al-Amoudi, A., Livolant, F., 2007. How to "read" a vitreous section. Methods Cell. Biol. 79, 385–406.

Dworkin, J., Shah, I.M., 2010. Exit from dormancy in microbial microorganisms. Nat. Rev. Microbiol. 8, 890–896. http://dx.doi.org/10.1038/nrmicro2453.

Eisenberg, B.R., Mobley, B.A., 1975. Size changes in single muscle fibers during fixation and embedding. Tissue Cell 7, 383–387.

Eltsov, M., Zuber, B., 2006. Transmission electron microscopy of the bacterial nucleoid. J. Struct. Biol. 156, 246–254. http://dx.doi.org/10.1016/j.jsb.2006.07.007.

Francesconi, S.C., MacAlister, T.J., Setlow, B., Setlow, P., 1988. Immunoelectron microscopic localization of small, acid-soluble spore proteins in sporulating cells of *Bacillus subtilis*. J. Bacteriol. 170, 5963–5967.

Frenkiel-Krispin, D., Minsky, A., 2006. Nucleoid organization and the maintenance of DNA integrity in *E. coli, B. subtilis* and *D. radiodurans*. J. Struct. Biol. 156, 311–319. http://dx.doi.org/10.1016/j.jsb.2006.05.014.

Frenkiel-Krispin, D., Sack, R., Englander, J., Shimoni, E., Eisenstein, M., Bullitt, E., Horowitz- Scherer, R., Hayes, C.S., Setlow, P., Minsky, A., Wolf, S.G., 2004. Structure of the DNA–SspC complex: implications for DNA packaging, protection, and repair in bacterial spores. J. Bacteriol. 6, 3525–3530. http://dx.doi.org/10.1128/JB.186.11.3525-3530.2004.

Fuchs, S., Hollins, A., Laue, M., Schaefer, U., Roemer, K., Gumbleton, M., Lehr, C.M., 2003. Differentiation of human alveolar epithelial cells in primary culture: morphological characterization and synthesis of caveolin-1 and surfactant protein-C. Cell Tissue Res. 311, 31–45. http://dx.doi.org/10.1007/s00441-002-0653-5.

Ghosal, S., Leighton, T.J., Wheeler, K.E., Hutcheon, I.D., Weber, P.K., 2010. Spatially resolved characterization of water and ion incorporation in *Bacillus* spores. Appl. Environ. Microbiol. 76, 3275–3282. http://dx.doi.org/10.1128/AEM.02485-09.

Hackett, H.R., Setlow, P., 1988. Properties of spores of *Bacillus subtilis* strains which lack the major small, acid-soluble protein. J. Bacteriol. 170, 1403–1404.

Han, H.M., Huebinger, J., Grabenbauer, M., 2012. Self-pressurized rapid freezing (SPRF) as a simple fixation method for cryo-electron microscopy of vitreous sections. J. Struct. Biol. 178, 84–87. http://dx.doi.org/10.1016/j.jsb.2012.04.001.

Han, H.M., Zuber, B., Dubochet, J., 2008. Compression and crevasses in vitreous sections under different cutting conditions. J. Microsc. 230, 167–171. http://dx.doi.org/10.1111/j.1365-2818.2008.01972.x.

Henriques, A.O., Moran Jr, C.P., 2007. Structure, assembly, and function of the spore surface layers. Ann. Rev. Microbiol. 61, 555–588. http://dx.doi.org/10.1146/annurev.micro.61.080706.093224.

Kong, L., Zhang, P., Wang, G., Yu, J., Setlow, P., Li, Y., 2011. Characterization of bacterial spore germination using phase-contrast and fluorescence microscopy, Raman spectroscopy and optical tweezers. Nat. Protoc. 6, 625–639. http://dx.doi.org/10.1038/nprot.2011.307.

Lane, H.C., La Montagne, J., Fauci, A.S., 2001. Bioterrorism: a clear and present danger. Nat. Med. 7, 1271–1273. http://dx.doi.org/10.1038/nm1201-1271.

Laue, M., Niederwöhrmeier, B., Bannert, N., 2007. Rapid diagnostic thin section electron microscopy of bacterial endospores. J. Microbiol. Meth. 70, 45–54. http://dx.doi.org/10.1016/j.mimet.2007.03.006.

Lee, K.S., Bumbaca, D., Kosman, J., Setlow, P., Jedrzejas, M.J., 2008. Structure of a protein–DNA complex essential for DNA protection in spores of *Bacillus* species. PNAS 105, 2806–2811. http://dx.doi.org/10.1073/pnas.0708244105.

Lepault, J., Dubochet, J., Baschong, W., Kellenberger, E., 1987. Organization of double-stranded DNA in bacteriophages: a study by cryo-electron microscopy of vitrified samples. EMBO J. 6, 1507–1512.

Luft, J.H., 1973. Embedding media – old and new. In: Koehler, J.K. (Ed.), Advanced Techniques in Biological Electron Microscopy. Springer, New York, Heidelberg, Berlin, pp. 1–34.

Mallozzi, M., Viswanathan, V.K., Vedantam, G., 2010. Spore forming Bacilli and Clostridia in human disease. Future Microbiol. 5, 1109–1123. http://dx.doi.org/10.2217/fmb.10.60.

Mason, J.M., Setlow, P., 1986. Essential role of small, acid-soluble spore proteins in resistance of *Bacillus subtilis* spores to UV light. J. Bacteriol. 167, 174–178.

McKenney, P.T., Driks, A., Eichenberger, P., 2013. The *Bacillus subtilis* endospore: assembly and functions of the multilayered coat. Nat. Rev. Microbiol. 11, 33–44. http://dx.doi.org/10.1038/nrmicro2921.

Minsky, A., Shimoni, E., Frenkiel-Kripsin, D., 2002. Stress, order and survival. Nature Rev. Mol. Cell Biol. 3, 50–60. http://dx.doi.org/10.1038/nrm700.

Mohr, S., Sokolov, N.V.H.A., He, C., Setlow, P., 1991. Binding of small acid-soluble spore proteins from *Bacillus subtilis* changes the conformation of DNA from B to A. PNAS 88, 77–81.

Nicholson, W.L., Setlow, B., Setlow, P., 1990. Binding of DNA in vitro by a small, acid-soluble spore protein from *Bacillus subtilis* and the effect of this binding on DNA topology. J. Bacteriol. 172, 6900–6906.

Pohanka, M., Kuca, P., 2010. Biological warfare agents. In: Luch, A. (Ed.), Molecular, Clinical and Environmental Toxicology, vol. 2. Birkhäuser, Basel, pp. 559–578.

Ragkousi, K., Cowan, A.E., Ross, M.A., Setlow, P., 2000. Analysis of nucleoid morphology during germination and outgrowth of spores of *Bacillus* species. J. Bacteriol. 182, 5556–5562. http://dx.doi.org/10.1128/JB.182.19.5556-5562.2000.

Roth, J., Taatjes, D.J., Tokuyasu, K.T., 1990. Contrasting of Lowicryl K4M thin sections. Histochemistry 95, 123–136. http://dx.doi.org/10.1007/BF00266584.

Santo, L., Doi, R.H., 1974. Ultrastructural analysis during germination and outgrowth of *Bacillus subtilis* spores. J. Bacteriol. 120, 475–481.

Setlow, B., Hand, A.R., Setlow, P., 1991. Synthesis of a *Bacillus subtilis* small, acid-soluble spore protein in *Escherichia coli* causes cell DNA to assume some characteristics of spore DNA. J. Bacteriol. 173, 1643–1653.

Setlow, B., Swaroopa, A., Kitchel, R., Koziol-Dube, K., Setlow, P., 2006. Role of dipicolinic acid in resistance and stability of spores of *Bacillus subtilis* with or without DNA-protective alpha/beta-type small acid-soluble proteins. J. Bacteriol. 188, 3740–3747. http://dx.doi.org/10.1128/JB.00212-06.

Setlow, P., 1995. Mechanisms for the prevention of damage to DNA in spores of *Bacillus* species. Ann. Rev. Microbiol. 49, 29–54. http://dx.doi.org/10.1146/annurev.mi.49.100195.000333.

Setlow, P., 2007. I will survive: DNA protection in bacterial spores. Trends Microbiol. 15, 172–180. http://dx.doi.org/10.1016/j.tim.2007.02.004.

Sterlini, J.M., Mandelstam, J., 1969. Commitment to sporulation in *Bacillus subtilis* and its relationship to development of Actinomycin resistance. Biochem. J. 113, 29–37.

Wolf, S.G., Frenkiel, D., Arad, T., Finkel, S.E., Kolter, R., Minsky, A., 1999. DNA protection by stress-induced biocrystallization. Nature 400, 83–85. http://dx.doi.org/10.1038/21918.